Constraints on the measurement of extension in the brittle upper crust

NICKY WHITE

White, N.: Constraints on the measurement of extension in the brittle upper crust. *Norsk Geologisk Tidsskrift*, Vol. 67, pp. 269–279. Oslo 1987. ISSN 0029-196X.

A general model is used to derive analytical expressions relating the shape of a normal fault and the shape of the sedimentary horizons in its hanging wall. The model assumes that: (1) The hanging wall block deforms by arbitrarily inclined simple shear; and (2) the footwall remains undeformed, though it may undergo rigid rotation. Differential compaction of hanging wall sediments due to burial while deformation takes place can be incorporated. The usual assumption that simple shear within the hanging wall block should occur on vertical planes is unjustified and it is argued here that simple shear is more likely to be inclined towards the footwall. Thus the horizontal displacement across a normal fault will not, in general, be equal to the amount of extension which has taken place. Hence the well-known discrepancy between the amount of extension obtained by summing horizontal displacements across normal faults and that obtained by other standard methods can be resolved.

Nicky White, BIRPS, Bullard Laboratories, Madingley Road, Cambridge CB3 0EZ, U.K.

It is now generally accepted that large-scale lithospheric stretching, as proposed by McKenzie (1978), can explain the formation of many continental sedimentary basins and margins. However, estimates of amounts of stretching obtained from measurements of crustal thickness and subsidence are often difficult to reconcile with those obtained from the observed normal faulting (see, for example, de Charpal et al. 1978; Le Pichon & Sibuet 1981; Wood & Barton 1983; Ziegler 1983). Usually this discrepancy is resolved by employing a more sophisticated stretching model than that which was originally proposed (Hellinger & Sclater 1983; Rowley & Sahagian 1986; Steckler 1985; Ziegler 1982). It is, however, possible that at least some of this discrepancy is due not to the inapplicability of the simple stretching model, but to significant underestimates of extension in the brittle upper crust. Clearly, a better understanding of the geometry and kinematics of the large-scale normal faults which accommodate the extension is first required before it can be determined whether or not the simple stretching model is appropriate.

Attempts to constrain fault geometry are often made by studying the faults themselves, using either field data or seismic reflection data (Wernicke & Burchfiel 1982; Anderson et al. 1983; Smith & Bruhn 1984). Seismological observations of earthquakes generated by active normal faults have also been used (Jackson & McKenzie 1983; Jackson in press). This paper is concerned with a different approach to the same problem – the detailed relationship between the geometry of a normal fault and the sediments in its hanging wall. This will clearly be strongly dependent on the nature of the deformation within the hanging wall block. Simple shear is shown to be the most likely form that this deformation takes. The analytic solution outlined is a simplified version of that derived by White et al. (1986). It differs from the usual graphical methods (Verrall 1981; Gibbs 1983, 1984) since it makes no assumption about the inclination of the shear planes. Allowances for compaction of hanging wall sediments and footwall rotation may also be made. The implications that this generalized model has for the determination of amounts of extension in the brittle upper crust are discussed.

Relating fault and bed geometries

The nature of the deformation

If a normal fault is non-planar, it is clear that the hanging wall must deform pervasively in order to accommodate movement along the fault, other-

wise voids will form. Coherent rotation of the hanging wall block is inadequate since it simply transfers the space problem further along the fault as Freeth & Lapido (1986) have pointed out. There are two possible forms that this deformation might take: (1) Flexural-slip folding; (2) similar or shear folding (see comprehensive review by Ramsay (1967)). In each case the footwall is assumed to remain rigid and undeformed.

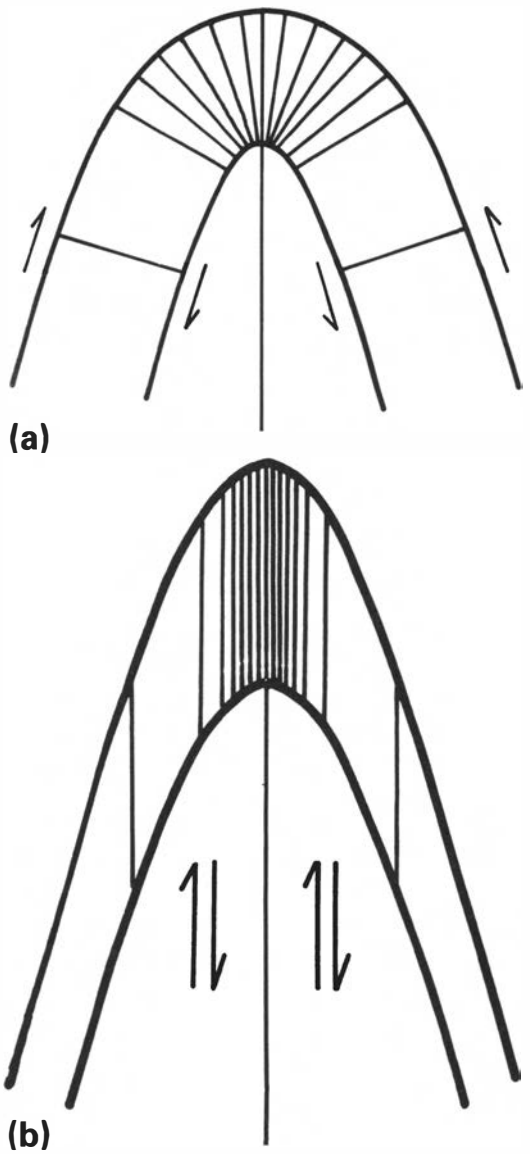

Fig. 1. (a) Flexural-slip fold formed by simple shear parallel to bedding. Bed length and orthogonal thickness are constant. Lines of constant dip, drawn every 10°, fan around the fold axis. (b) Similar or shear fold formed by inhomogeneous simple shear at a high angle to bedding. In the limbs, as shearing proceeds, bed length increases and orthogonal thickness decreases. Lines of constant dip are drawn every 10° parallel to the fold axis. Both diagrams are redrawn from Ramsay (1967).

Large-scale flexural-slip folds can only develop in rocks with a well-developed plane-parallel stratification. As folding proceeds (Fig. 1a), the individual layers are flexed such that the uppermost slip over the lower towards the fold axis. Fig. 2 shows a flexural-slip fold that has formed over a listric normal fault which, for simplicity, becomes planar and horizontal with depth. Cross-sectional area is preserved. In addition, bed-length together with orthogonal thickness remain constant. Thus the section is balanced in the sense of Dahlstrom (1969). There is no simple relationship between extension and the horizontal displacement or heave across the fault. However, the amount of extension is invariably less than the heave or, equivalently, the slip along the fault itself decreases as fault dip decreases.

Shear folds can occur in the presence or absence of well-developed stratification. They often form as a result of progressive, inhomogeneous simple shear (Fig. 1b). The shear planes may be infinitely close and are not necessarily visible in naturally deformed rock (Ramsay 1967). The development of a shear fold in the hanging wall of a normal fault can be considered in two steps, although the process is actually continuous. Firstly, as illustrated in Fig. 3a, the hanging wall block displaces horizontally to produce a void. In order to fill the void, the hanging wall block then deforms by simple shear (Fig. 3b). This shear is usually assumed to occur along vertical planes, though

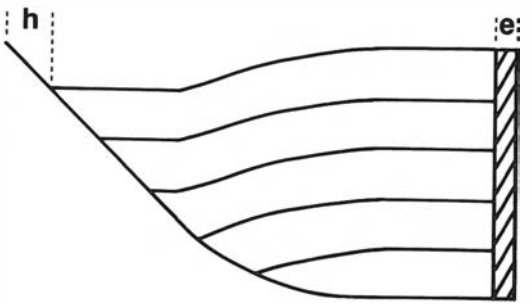

Fig. 2. The hanging wall has deformed by flexural-slip folding to accommodate motion along the fault. The amount of inter-bed slip increases as dip increases. None will occur if the beds remain horizontal. The amount of extension, ε, can be empirically determined from the heave, h, and is always less than h.

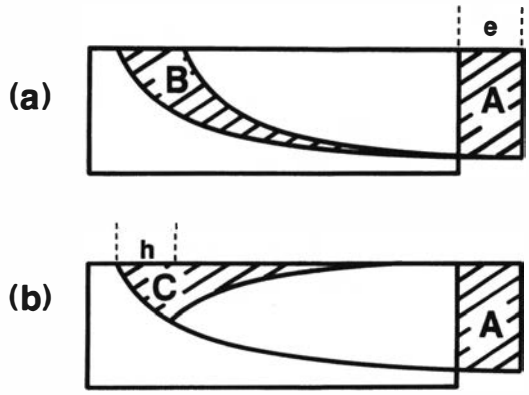

Fig. 3. Illustration of how the hanging wall deforms by simple shear. Firstly, the hanging wall is displaced causing a void to form area B. It then deforms by simple shear to fill this void. Clearly areas A, B and C are all equal. The horizontal displacement across the fault, i.e. the heave, *h*, is only equal to the extension, e, when the void fills by *vertical* shear.

there is no particular reason why this should be so. Cross-sectional area is preserved. Bed-length does not remain constant and the orthogonal thickness of beds decreases with the dip of the strata (Fig. 4). A simple relationship between extension and heave can be derived. Depending on the inclination of the shear planes, the amount of extension is greater or less than the heave (see below).

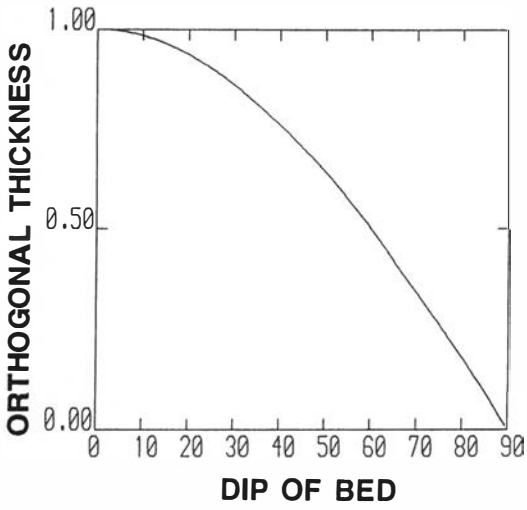

Fig. 4. Decrease of orthogonal thickness with increasing dip of bed for the simple shear model. If the dip is 0°, then there is no change in the orthogonal thickness. For a dip of 45°, the orthogonal thickness decreases to about 0.7.

Both the flexural-slip model and the simple shear model can be used to predict fault geometries and, thus, determine amounts of extension (Davison 1986; Verrall 1981). The flexural-slip model has a number of disadvantages, however:

(1) Antithetic faulting is often observed within the hanging wall block. Since this disrupts layering it will inhibit inter-bed slip.

(2) Syntectonic burial of hanging wall sediments can result in differential compaction. This process involves sub-vertical inhomogeneous shearing which will also hinder the folding mechanism.

(3) Thickness variations such as those which occur as a result of growth-type faulting may cause problems since plane-parallel stratification is required for efficient inter-bed slip (Ramsay 1967).

It is not clear how the flexural-slip model can be reconciled with these commonly observed features. Therefore it will not be considered any further although there may be circumstances when small amounts of inter-bed slip do occur. As shown below, a generalized simple shear model can easily incorporate the above observations.

A general model

Verrall (1981) used a simple graphical technique to relate fault and sediment geometries. This method implicitly assumes that the hanging wall block deforms by simple shear in vertical planes. The other main assumptions are:

(1) There is no movement out of the plane of the section.
(2) The footwall remains completely rigid throughout.
(3) Sediment geometry has not been altered by compaction.

Subsequently, White et al. (1986) derived a general solution which does not fix the inclination of the planes along which simple shear occurs and which can be modified to include compaction and footwall rotation. A simplified version of this solution will now be discussed.

The forward problem – from fault to bed geometry

Consider the deformation of the hanging wall in a co-ordinate system fixed to the footwall (Fig.

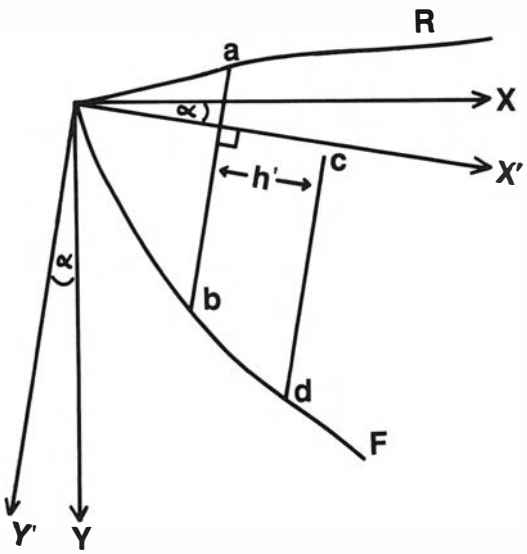

Fig. 5. Co-ordinate system and geometrical relationships used to derive equation (2).

5). The planes along which simple shear occurs are parallel to the y' direction, which is not, in general, perpendicular to the earth's surface. In this frame, $B' = B'(x')$ and $F' = F'(x')$ are the y' co-ordinates of the bed and the fault respectively. Let us assume that prior to deformation the bed had an initial shape or 'regional' given by $R' = R'(x)$. An element $|ab|$ of the hanging wall block now moves a distance h' in the x' direction such that point a moves to point c and b moves to d.

The co-ordinates of the points a, b, c and d are:

$$\begin{aligned} a &= (x', R'(x')) \\ b &= (x', F'(x')) \\ c &= (x' + h', B'(x' + h')) \\ d &= (x' + h', F'(x' + h')) \end{aligned} \tag{1}$$

No voids are allowed to form so clearly $|ab| = |cd|$, which implies that

$$B'(x' + h') = F'(x' + h') - F'(x') + R'(x') \tag{2}$$

Equation (2) is in the (x', y') co-ordinate frame, where simple shear is in the y' direction. But the (x', y') frame is rotated through some angle α with respect to the (x, y) frame where y is the vertical direction. Therefore the fault F and the regional R, defined in the (x, y) frame, must be rotated into the (x', y') frame using the relations:

$$\begin{aligned} x' &= x \cos \alpha + y \sin \alpha \\ y' &= -x \sin \alpha + y \cos \alpha \end{aligned} \tag{3}$$

where y is F or R. h' must also be calculated by rotating the heave known in the (x, y) frame into the (x', y') frame. The bed, B', can then be calculated at each point, $x' + h'$, for a range of values of x'. B' is returned to the (x, y) frame using the relations:

$$\begin{aligned} x &= x' \cos \alpha - y' \sin \alpha \\ y &= x' \sin \alpha + y' \cos \alpha \end{aligned} \tag{4}$$

Given the fault geometry, F, and the heave, h, it is clear that a whole range of bed shapes can be calculated depending upon the value of α. The effect of varying α is illustrated in Fig. 6. A fault with dog-leg geometry is used, the two legs being joined by the arc of a circle. For simplicity $R = 0$. Three different values of α have been used. In each case, the bed geometry constructed is clearly very different, even though the heave is the same. Similarly, the area of the depression in each hanging wall is different. If $\alpha = 0°$ then the amount of extension or slip along the horizontal portion of the fault is equal to the heave (Fig. 6(b)). But when $\alpha \neq 0°$ it is clear from the vectors drawn in Figs. 6(a) and (c) that the amount of extension, ε, will not be equal to h. In fact, White et al. (1986) show that

$$\varepsilon = h(1 + \tan \theta \tan \alpha) \tag{5}$$

where θ is the dip of the fault. If $\alpha = -30°$ and $\theta = 45°$ then $\varepsilon = 0{\cdot}4h$, whereas if $\alpha = +30°$ then $\varepsilon = 1{\cdot}6h$. Thus the amount of extension may be greater or less than the heave depending on whether α is positive or negative. Increasing α must also increase the area of the depression in the hanging wall block since this is simply the extension multiplied by the depth at which the fault flattens out (Gibbs 1983). The implications of these simple calculations will be discussed in more detail below.

The inverse problem – from bed to fault geometry

From equation (2) we have

$$F'(x' + h') = F'(x') - R'(x') + B'(x' + h') \tag{6}$$

Thus, given the bed geometry, the initial dip of the fault at the surface and the heave, many

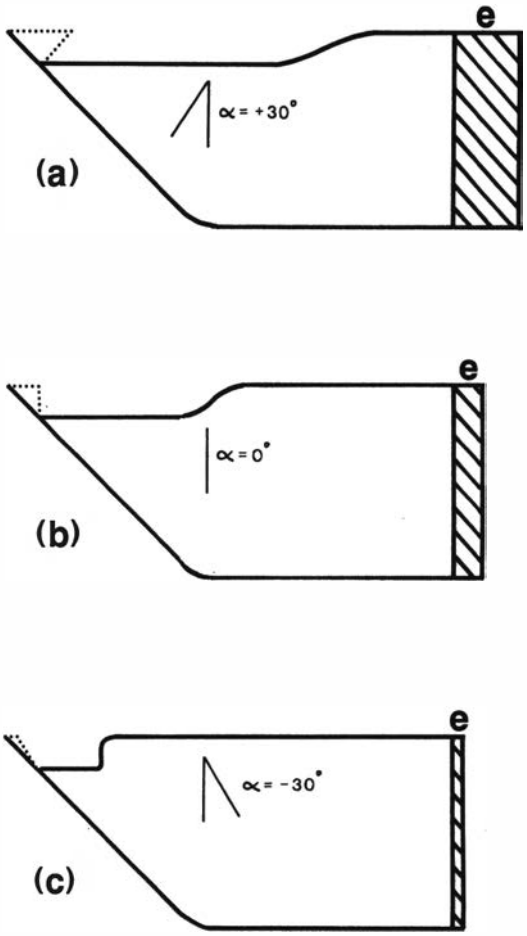

Fig. 6. Illustration of the forward problem using a dog-leg fault whose segments, dipping at 45° and 0°, are linked by the arc of a circle. The shape of a bed within the hanging wall is shown for three different values of α. The heave is identical in each case. (a) $\alpha = +30°$. The hanging wall first translates by an amount ε. It then shears towards the footwall as indicated. The amount of shear that occurs decreases as the dip of the fault decreases. When the dip of the fault is zero, no shearing occurs and the hanging wall block simply translates by an amount ε. Clearly the heave, h, is less than the extension, ε. (b) Shearing is vertical ($\alpha = 0°$). Thus $\varepsilon = h$. (c) $\alpha = -30°$. The direction of shear is now the complete opposite of that in (a). As a result, h is much less than ε.

different faults can be constructed depending on the value of α, the inclination of the simple shear. In Fig. 7 the fault geometries for $\alpha = -30°$, $\alpha = 0°$ and $\alpha = +30°$ are shown. The bed geometry used is identical to that in Fig. 6(b). An increase in α causes the fault to flatten out at a shallower depth. For a given α only one bed is needed to calculate the fault geometry. Similarly, if the

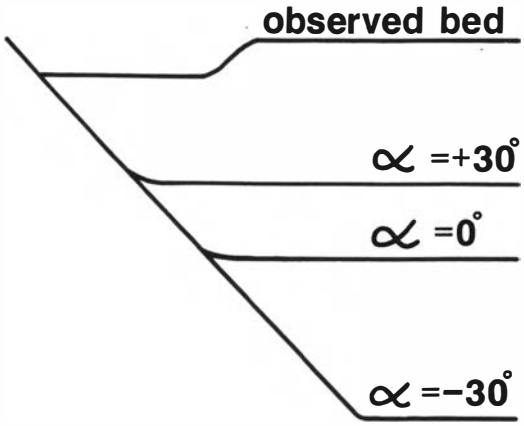

Fig. 7. Illustration of the inverse problem. Three different fault geometries are predicted for the same observed bed shape and heave. As α increases from $-30°$ to $+30°$, the depth to decollement decreases.

fault, F, is known, then α can be determined. In general, however, both F and α are unknown and a unique solution cannot be found using the geometry of just one bed. F and α are common to all beds in the hanging wall block. So, if the geometries of two beds are known then we will have two equations but still only two unknowns. A solution to the two equations can be found as follows: For any given value of α, two different faults can be calculated – one for each bed. The difference between these two faults, i.e. the area A shown in Fig. 8, will vary with α. Thus A is a

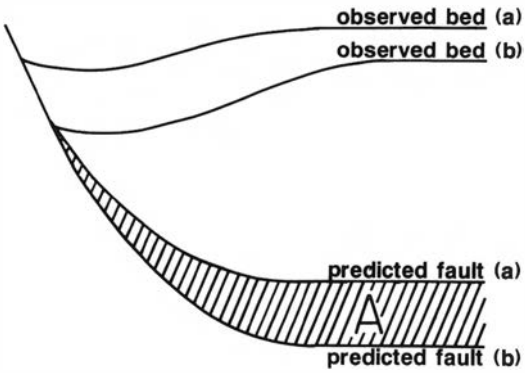

Fig. 8. The general inverse problem. Two beds (a) and (b) are known. The fault, F, and the angle of simple shear, α, are unknown. For a given value of α, fault (a) is calculated from bed (a) and fault (b) from bed (b). The area, A, between the two faults will vary depending upon the value of α. F and α are found when the function A is minimized.

function of α which can be minimized to yield the required solution (White, in prep.).

Footwall deformation

The most important assumption inherent in equation (2) is that the footwall remains undeformed. Some justification for this comes from seismological studies of earthquakes generated by active normal faults in regions such as the Aegean (Jackson et al. 1982; Jackson 1987). There, the sequences of aftershocks which follow large magnitude events are largely confined to hanging wall blocks. Some do occur in footwall blocks, but their cumulative seismic moment is insignificant compared to that of the main shock (King et al. 1985). The methods described in this paper should thus work reasonably well down to a depth of about 10 km (the maximum depth at which earthquakes nucleate). Below this depth the footwall may experience some form of distributed deformation.

The problem of footwall rotation may be encountered when applying equations (2) and (6) to major faults. Large-scale rotation of crustal blocks about a horizontal axis is necessary if the motion along faults (simple shear) is to be converted into pure shear, i.e. stretching (McKenzie & Jackson 1983). Field observations confirm this notion (Ransome et al. 1910; Morton & Black 1975). Allowance for rotation can be made by setting the initial dip or 'regional' of the beds equal to the amount of rotation. Thus

$$R(x) = x \tan \omega \tag{7}$$

where ω is the rotation.

Compaction

The model

Sediments within the hanging wall of a large-scale normal fault may contain considerable amounts of water. As deformation and burial take place, this water is expelled and the sediments compact. It is important to determine the effect that compaction has on (a) the forward problem and (b) the inverse problem. This is done here by using a simplified version of the expression derived by White et al. (1986).

Most workers assume that the strain caused by compaction is uniaxial, the axis of shortening being vertical. This assumption is reasonable provided that lateral changes in facies and thickness of sedimentary layers can be neglected. However, it is unlikely to be an accurate description of the strain field in a region which is undergoing burial and tectonic deformation at the same time. The equations governing the behaviour of such a system have recently been derived by McKenzie (1984).

No attempt has been made here to solve this more general problem. Instead, the standard expression which relates porosity to depth (Magara 1978; Sclater & Christie 1980; Steckler & Watts 1978) has simply been modified. The resulting equation only yields an approximate solution to the full problem and, for this reason, should be applied with care.

Equations derived previously assume that the hanging wall deforms by simple shear alone. If the strain field is more complicated, such equations do not hold. This situation is avoided by constraining the strain field produced by compaction to be uniaxial with the axis of shortening parallel to the shear direction within the hanging wall. This is unlikely to be any worse than assuming that compaction occurs by uniaxial shortening in a purely vertical direction (White in prep). Throughout, it is assumed that the footwall does not compact. This is only strictly true when the footwall has not been covered with sediment. When it has, the following equations must be modified slightly.

The porosity at any depth, d, is

$$\phi = \phi_0 \exp\left\{\frac{-d}{\lambda}\right\} \tag{8}$$

where ϕ_0 is the initial porosity and λ is a constant governing the change of porosity with depth. As before, the (x', y') co-ordinate frame is rotated through an angle, α, with respect to the (x, y) frame. Thus the porosity at any point in the (x', y') frame is

$$\phi' = \phi_0' \exp\left\{\frac{-d'}{\lambda'}\right\} \tag{9}$$

where ϕ_0' is the initial porosity and λ' is the depth constant, both determined in the rotated frame. As before, with reference to Fig. 5, consider four points a, b, c and d. The length $|ab|$ will compact as it moves down the fault. Therefore, $|ab|$ will no longer be equal to $|cd|$. The amount of solid material between points a and b will, however,

be the same as that between points c and d. Thus:

$$\int_a^b (1-\phi')dy' = \int_c^d (1-\phi')dy' \qquad (10)$$

Substitution of equations (1) into (10) followed by integration yields:

$$F'(x'+h') = F'(x') - R'(x') + \phi_0'\lambda'\left\{\exp\left(\frac{-F'(x')}{\lambda'}\right) - \exp\left(\frac{-R'(x')}{\lambda'}\right)\right\} + B'(x'+h') - \phi_0'\lambda'\left\{\exp\left(\frac{-F'(x'+h')}{\lambda'}\right) - \exp\left(\frac{-B'(x'+h')}{\lambda'}\right)\right\} \qquad (11)$$

This equation may be solved by iteration either for F when B is given or for B when F is given. When $\phi_0 = 0$, equation (11) is identical to equation (6). This provides an initial solution to (11). About ten iterations are then needed to find the correct answer.

Examples and implications

The forward problem. – Fig. 9 shows the effect that compaction has in two different situations. In Figs. 9a & 9b the beds were deposited, and therefore partially compacted, prior to deformation. As a result of faulting, beds close to the surface outcrop of the fault are more deeply buried than those further away in the hanging wall block. Therefore, beds closest to the surface expression of the fault compact the most. The effect on bed geometry is greater for shallow beds since deeper ones have lost most of their porosity before faulting. Figs. 10a & 10b show the effect of compaction on beds that were deposited at different stages during faulting. In this case compaction causes a pronounced downwarping of beds, i.e. a 'hanging wall syncline'. This is similar to 'normal drag' (Hobbs et al. 1976), except that it has a longer wavelength. The presence of features similar to those illustrated is a good indication that the effects of compaction are significant and should be allowed for.

The inverse problem. – The effect that compaction may have on the inverse problem is illustrated in Fig. 11. Here a compacted bed is used to calculate the fault geometry without allowing for compaction. The result is an initially convex-upwards fault whereas the fault is, in fact, planar. This clearly indicates that compaction should not be ignored.

In equation (6), there were just two unknowns, F and α.

Equation (11) has four – F, α, ϕ_0 and λ. When (11) is applied to a particular data set, one or

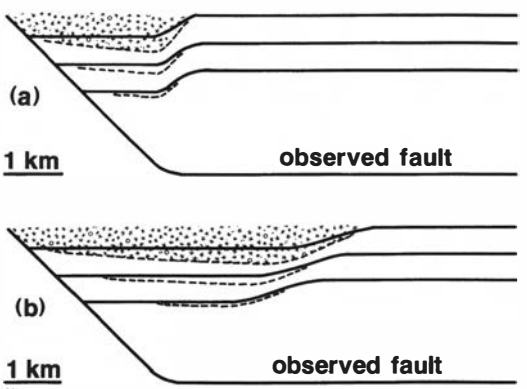

Fig. 9. Bed geometries have been calculated for a given fault with compaction effects taken into account. All three beds represented by solid lines were deposited and thus partially compacted prior to faulting. Motion along the fault causes a depression to form in the hanging wall. This alone fills with sediment (dotted) causing the original beds to compact further. Note that the deepest bed compacts less than the shallowest one since it was already partially compacted. Two different values of α have been used: (a) $\alpha = 0°$ and (b) $\alpha = 45°$. In both cases $\phi_0 = 0{\cdot}6$ and $\lambda = 2$ km.

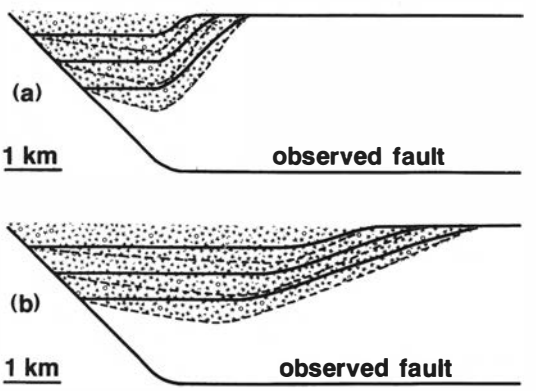

Fig. 10. This is similar to Fig. 9. The difference is that all the beds shown were deposited *during* faulting, i.e. it is a growth fault. After each increment in slip, the depression formed fills with sediment causing deeper beds, which were originally at the surface, to compact. Note that the effect of compaction increases with depth, whereas in Fig. 9 it decreased with depth. Two different values of α have been used: (a) $\alpha = 0°$ and (b) $\alpha = 45°$. In both cases $\phi_0 = 0.6$ and $\lambda = 2$ km.

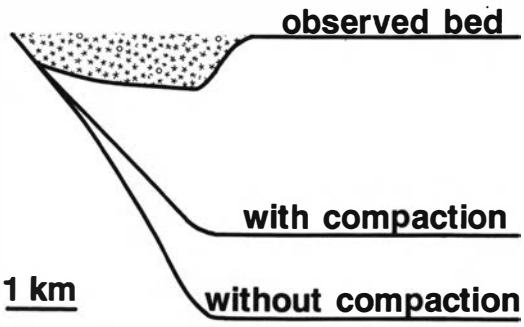

Fig. 11. Illustration of the inverse problem where fault geometry is calculated given a compacted bed geometry. When compaction is neglected, a fault with a convex-upwards bulge is predicted. The correct fault is calculated when compaction is taken into account. Parameters as in Fig. 10(a).

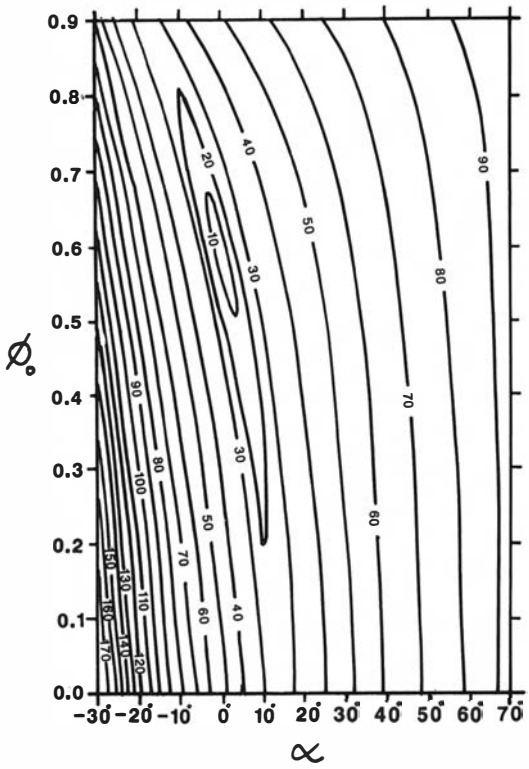

Fig. 12. The area, A, between two faults calculated from two beds is a function of α, ϕ_0 and λ (see text and Fig. 8). Here, a contour map of the variation of A with respect to α and ϕ_0 is shown. λ was chosen to be 2 km. A strong global minimum is present and the function is approximately quadratic. At the minimum, $\alpha = 0°$ and $\phi_0 = 0.6$. Changes in λ and in the fault/bed geometry do not significantly alter the form of A.

more of these variables may be fixed though in general this is not the case. Fortunately, the geometry of the fault can always be determined provided at least two beds are known. As before, each bed is used to calculate a fault for any given values of the variables. This time the area, A, between the two faults is a function of *three* parameters: α, ϕ_0 and λ.

A number of important observations can be made about the form taken by this empirical function, $A(\alpha, \phi_0, \lambda)$ (Fig. 12). The most notable is that it is both smooth and approximately quadratic. It also has a very strong global minimum (Scales 1985). The required values of α, ϕ_0 and λ are the co-ordinates of this minimum point. A is much more strongly dependent upon α than upon ϕ_0 or λ. This is very significant since it implies that the value of α obtained when compaction is ignored is still close to the true value. Thus, even though White et al. (1986) did not take compaction into account in their examples, the values they obtained for α are approximately correct. The form that $A(\alpha, \phi_0, \lambda)$ takes does not change very much for different bed and fault geometries (White in prep.).

When equation (11) is applied to data, the function $A(\alpha, \phi_0, \lambda)$ must be minimized. Values for α, ϕ_0 and λ can then be obtained and the geometry of the fault calculated. Finding the minimum is best done using one of the many algorithms now available (Scales 1985; White in prep.).

Inclined shear

So far, nothing has been said about what values α, the inclination of simple shear, can have. Usually α is assumed to be zero (Gibbs 1983, 1984). However, White et al. (1986) argue that this need not necessarily be the case. Their examples, taken from seismic reflection profiles, suggest that α usually has values between +30° and +45°, i.e. shear is inclined towards the footwall. Although they ignored compaction, it is clear from Fig. 11 that this will have a small effect on the angles of simple shear they obtained.

Positively inclined shear is entirely consistent with the observation that antithetic faults in hanging wall blocks are rarely vertical (Okaya & Thompson 1985). The deformation within the hanging wall blocks of active normal faults in the Aegean also occurs along inclined antithetic faults (Jackson et al. 1982; King et al. 1985). Negative

values of α have never been observed. This is to be expected since negative α would mean that the hanging wall was actually *shortening*.

If the value of α is changed from 0° to 30° the predicted fault geometry changes considerably (Fig. 7). For a calculated fault which becomes horizontal at some depth, d, increasing α will make d smaller since

$$d = \frac{p}{h(1 + \tan\theta \tan\alpha)} \qquad (12)$$

where p is the area of the depression which forms due to deformation in the hanging wall block.

This is significant because Bosworth (1985) found that applying the vertical shear model often gives very large values for d which cannot be reconciled with geological observation. The problem is resolved if inclined shear is adopted.

Calculating extension

Estimates of extension obtained from measurements of crustal thickness and subsidence are considerably greater than those obtained from normal faulting (Steckler 1985; Wood & Barton 1983; Ziegler 1983). Before the significance of this discrepancy can be assessed, it is essential to determine how well upper crustal extension can be constrained. Usually, extension is estimated by measuring the heave across each normal fault (Ziegler 1982). As pointed out above, the heave, h, is only equal to the extension, ε, when the angle of simple shear, α, is zero. For positive values of α, ε may be considerably greater than h. Fig. 13 shows ε/h as a function of θ, the dip of the fault at the surface, and α. The dip of the fault at depth is assumed to be zero. Given $\theta = 45°$, increasing α from 0° to 45° will double ε/h. Higher values of θ and α increase ε/h even more.

When footwall rotation occurs, a different method must be used to calculate extension (Fig. 14, White in prep.). In this case the significant parameters are the final dip of the fault at the surface, θ, the final dip of the fault at depth, σ, and the rotation, ω. σ must be calculated using equation (11), so it is strongly dependent upon α. For a planar fault dipping at 30° and a rotation of $\omega = 20°$, β (the stretching factor) is 1·5. Decreasing σ, the final dip of the fault at depth, to 15° increases β to 2·1 for the same rotation, $\omega = 20°$.

Figs. 13 and 14 both show that upper crustal extension can be significantly underestimated if the effect of inclined shear is ignored. Thus the much discussed discrepancy between amounts of upper crustal and lithospherical stretching in sedimentary basins such as the North Sea can be explained (White in prep).

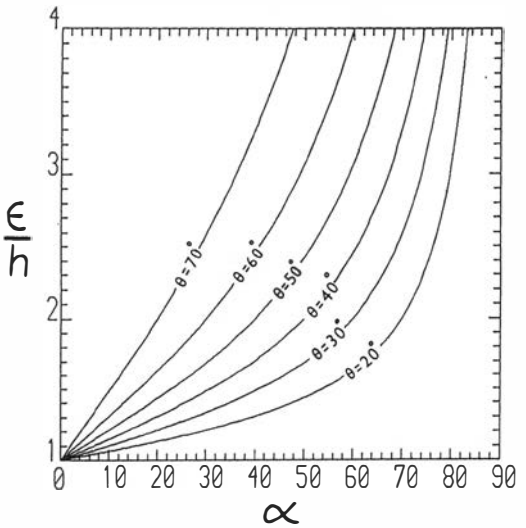

Fig. 13. The ratio of extension to heave is shown as a function of the initial dip of the fault, θ, and the angle of simple shear, α. When $\alpha = 0°$, then $\varepsilon = h$. As both α and θ increase, ε becomes significantly greater than h. The final dip of the fault is assumed to be zero and the footwall does not rotate.

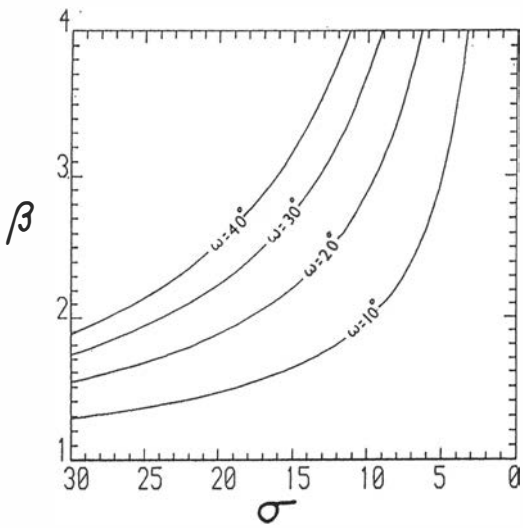

Fig. 14. The stretching parameter, β, is shown as a function of the amount of footwall rotation, ω, and the final dip of the fault at depth, σ. θ, the final dip of the fault at the surface, is 30°. When $\sigma = 30°$, the fault is planar and $\beta = 1.5$ when $\omega = 20°$. If σ decreases to 15° and ω stays the same, then $\beta = 2.1$. When $\sigma = 0°$, $\beta = \infty$.

Conclusions

Simple analytical expressions relating the shape of a normal fault in cross-section to the shape of the sedimentary horizons in its hanging wall block have been derived. These expressions assume that the hanging wall deforms by simple shear and that the footwall remains undeformed, though it may rotate. Simple shear may potentially be inclined at any angle. However, it is argued here that values of about 45° can be expected. Similar estimates have been obtained by White et al. (1986) using seismic reflection data.

A simple approximation is used to account for syntectonic compaction of hanging wall sediments. This usually causes a pronounced downwarping of sediments close to the footwall. If such 'hanging wall synclines' are used to calculate fault geometry, without allowing for compaction, the predicted fault geometry is quite different. Although compaction is clearly an important effect, whether it is taken into account or not will not significantly alter the calculated value of α, the inclination of simple shear.

Usually, the amount of extension across a normal fault is assumed to be equal to the horizontal displacement across the fault, i.e. the heave. However, for non-planar faults and positive values of α this will not be the case. Extension can, in fact, be several times greater than the heave. Thus usual measurements of regional extension in sedimentary basins such as the North Sea may be significant underestimates.

Acknowledgements. – I am very grateful to Dan McKenzie for his enthusiastic help and encouragement. Bernard Raynaud stopped me from going wildly astray at a very early stage and Mike Cheadle subjected an early version of the script to friendly but penetrating criticism. I thank the British Council for an F.C.O. studentship and Merlin Geophysical for very generous support. Cambridge University Department of Earth Sciences contribution no. 989.

References

Anderson, R. E., Zoback, M. L. & Thompson, G. A. 1983: Implications of selected sub-surface data on the structural form and evolution of some basins in the northern Basin and Range Province, Nevada and Utah. *Bulletin of the Geological Society of America 94,* 1055–1972.

Bosworth, W. 1985: *Discussion* on the structural evolution of extensional basin margins. *Journal of the Geological Society of London 142,* 939–942.

de Charpal, O., Guennoc, P., Montadert, L. & Roberts, D. G. 1978: Rifting, crustal attenuation and subsidence in the Bay of Biscay. *Nature (London) 275,* 706–711.

Dahlstrom, C. D. A. 1969: Balanced cross-sections. *Canadian Journal of Earth Science 6,* 743–757.

Davison, I. 1986: Listric normal fault profiles: calculation using bed-length balance and fault displacement. *Journal of Structural Geology 8,* 2, 209–210.

Freeth, S. J. & Lapido, K. O. 1986: The development and restoration of syn-sedimentary faults. *Earth and Planetary Science Letters 80,* 411–419.

Gibbs, A. D. 1983: Balanced cross-section construction from seismic sections in areas of extensional tectonics. *Journal of Structural Geology 5,* 153–160.

Gibbs, A. D. 1984: Structural evolution of extensional basin margins. *Journal of the Geological Society of London 141,* 609–620.

Hellinger, S. J. & Sclater, J. G. 1983: Some comments on two-layer extension models for the evolution of sedimentary basins. *Journal of Geophysical Research 88,* B10, 8251–8269.

Hobbs, B. E., Means, W. D. & Williams, P. F. 1976: *An Outline of Structural Geology,* John Wiley & Sons, New York.

Jackson, J. A. 1987: Active normal faulting and crustal extension. *In* Coward, M. P., Dewey, J. F. & Hancock, P. L. (eds.): Continental Extensional Tectonics. *Geological Society of London Special Publication No. 28,* 3–17.

Jackson, J. A. & McKenzie, D. P. 1983: The geometrical evolution of normal fault systems. *Journal of Structural Geology 5,* 471–482.

Jackson, J. A., King, G. & Vita-Finzi, C. 1982: The neotectonics of the Aegean: an alternative view. *Earth and Planetary Science Letters 61,* 303–318.

King, G. C. P., Ouyang, Z. X., Papadimitriou, P., Deschamps, A., Gagnepain, J., Houseman, G., Jackson, J. A., Soufleris, C. & Virieux, J. 1985: The evolution of the Gulf of Corinth (Greece): an aftershock study of the 1981 earthquakes. *Geophysical Journal of the Royal Astronomical Society 80,* 677–693.

Le Pichon, X. & Sibuet, J. C. 1981: Passive margins: a model of formation. *Journal of Geophysical Research 86,* 3708–3721.

Magara, K. 1978: *Compaction and Fluid Migration.* Dev. Pet. Sci. *9,* Elsevier, New York.

McKenzie, D. P. 1978: Some remarks on the development of sedimentary basins. *Earth and Planetary Science Letters 40,* 25–32.

McKenzie, D. P. 1984: The generation and compaction of partial melts. *Journal of Petrology 25,* 713–765.

McKenzie, D. P. & Jackson, J. A. 1983: The relationship between strain rates, crustal thickening, palaeomagnetism, finite strain and fault movements within a deforming zone. *Earth and Planetary Science Letters 65,* 182–202.

Morton, W. H. & Black, R. 1975: Crustal attenuation in Afar. *In* Pilger, A. & Rosler, A. (eds.): *Afar Depression of Ethiopia,* 55–65. Inter-union commission on geodynamics. Scientific Report Number 14. E. Schweizerbart'sche Verlagsbuchhandlung, Stuttgart.

Okaya, D. A. & Thompson, G. A. 1985: Geometry of Cenozoic extensional faulting: Dixie Valley, Nevada. *Tectonics 4,* 1, 107–126.

Ramsay, J. G. 1967: *Folding and Fracturing of Rocks.* McGraw-Hill Book Company, San Francisco.

Ransome, F. L., Emmons, W. H. & Garrey, G. H. 1910: Geology and ore deposits of the Bullfrog District, Nevada. *Bulletin of the United States Geological Survey 407.*

Rowley, D. B. & Sahagian, D. 1986: Depth-dependent stretching: A different approach. *Geology 14,* 32–35.

Scales, L. E. 1985: *Introduction to Non-linear Optimization,*

243 pp. Macmillan Publishers Ltd., London and Basingstoke.

Sclater, J. G. & Christie, P. A. F. 1980: Continental stretching: An explanation of the post mid-Cretaceous subsidence of the Central North Sea. *Journal of Geophysical Research 85,* 3711–3739.

Smith, R. B. & Bruhn, R. L. 1984: Intraplate extensional tectonics of the eastern Basin-Range: Inferences on structural style from seismic reflection data, regional tectonics and thermal-mechanical models of the brittle-ductile deformation. *Journal of Geophysical Research 89,* 5733–5762.

Steckler, M. S. 1985: Uplift and extension at the Gulf of Suez: Indications of induced mantle convection. *Nature (London) 317,* 135–139.

Steckler, M. S. & Watts, A. B. 1978: Subsidence of the Atlantic margin of New York. *Earth and Planetary Science Letters 41,* 1–13.

Verrall, P. 1981: Structural interpretation with application to North Sea problems. Course notes No. 3, JAPEC (UK).

Wernicke, B. P. & Burchfiel, B. C. 1982: Modes of extensional tectonics. *Journal of Structural Geology 4,* 105–115.

White, N. J., Jackson, J. A. & McKenzie, D. P. 1986: The relationship between the geometry of normal faults and that of the sedimentary layers in their hanging walls. *Journal of Structural Geology 8,* 8, 879–909.

Wood, R. & Barton, P. 1983: Crustal thinning and subsidence in the North Sea. *Nature (London) 302,* 134–136.

Ziegler, P. A. 1982: Faulting and graben formation in western and central Europe. *Philosophical Transactions of the Royal Society of London A 305,* 113–143.

Ziegler, P. A. 1983: Crustal thinning and subsidence in the North Sea. *Nature (London) 304,* 561.